BNL-61817

JOURNAL OF GEOPHYSICAL RESEARCH, VOL. 101, NO. D22, PAGES 29,061–29,074, DECEMBER 20, 1996

Measurement of O_3 and related compounds over southern Nova Scotia 2. Photochemical age and vertical transport

Lawrence I. Kleinman,[1] Peter H. Daum,[1] Stephen R. Springston,[1] W. Richard Leaitch,[2] Catharine M. Banic,[2] George A. Isaac,[2] B. Thomas Jobson,[3] and Hiromi Niki[4,5]

Abstract. Chemical measurements of O_3 and other trace substances in the atmosphere over southern Nova Scotia, obtained during 48 flights of the National Research Council of Canada Twin Otter aircraft, provide evidence for a variable degree of processing associated with transport times ranging from less than 1 day to 5 days or more. Effects of chemical aging and dilution are determined using photochemical age estimates derived from the ratios, ln (n-butane/propane) and ln (i-butane/propane). Age estimates are used in a qualitative sense to divide the data set into four age groups. Vertical profiles and relations between O_3 and other trace substances are examined as a function of age group. We find that high-O_3 events occurring in dry air are in the oldest age category. Moist high-O_3 events have photochemical ages that span all four age categories, but the most polluted episodes are only observed in relatively "new air." A geographically wide range of emission regions is suggested by the hydrocarbon measurements, which is consistent with back trajectory results. The relative depletion of soluble substance (i.e., aerosol particles and NO_y) in dry, relative to moist, high-O_3 air masses is discussed with respect to the dilution or precipitation scavenging that must accompany the transport of pollutants from the boundary layer to the dryer middle or upper troposphere. Four case studies are presented that span a wide range of conditions associated with high O_3 concentrations. In a pair of these cases, samples were obtained in air masses having about the same photochemical age, altitude, and C_2H_2 and O_3 concentration. One of the pair was from dry air and the other from moist air. The dry air mass had much lower concentrations of NO_y and aerosol particles, which was interpreted as evidence for the selective removal of soluble constituents during vertical lifting. The other case studies illustrate a biomass burning plume and the effects of a stable layer over the ocean on transport.

1. Introduction

Atmospheric composition measurements made during the 1993 North Atlantic Regional Experiment (NARE) intensive document the wide range of conditions that occur at the surface and in the air over southern Nova Scotia [*Fehsenfeld et al.*, this issue (a, b)]. Meteorological conditions determine whether this region will be exposed to effluents from industrialized regions within North America or to much cleaner air coming from less populated areas located to the south, east, or north. Regions with high emission rates that can be upwind of Nova Scotia include relatively nearby areas such as Boston or New York City, as well as relatively remote regions in the interior of the United States and Canada. Central and northern Canadian regions with biomass burning, as documented in the ABLE 3B campaign [*Shipman et al.*, 1994], can also be upwind. As Nova Scotia is located hundreds to thousands of kilometers away from these emission regions, the composition of the air over Nova Scotia will reflect a variable and sometimes large degree of chemical and physical processing that occurs during transport.

In a preceding paper [*Kleinman et al.*, this issue] (hereinafter referred to as part 1), we presented chemical data on O_3, O_3 precursors, and anthropogenic tracers gathered from 48 flights of the National Research Council of Canada (NRC) Twin Otter aircraft. The data set derives primarily from vertical profiles and short horizontal traverses over the surface monitoring site at Chebogue Point, Nova Scotia, and over the Atlantic Ocean within 50 km of Chebogue Point. In part 1 we presented observations in a format which showed the day-to-day and altitude variations in chemical composition. We focused on the characteristics of high-O_3 events, finding distinct differences between these events in moist and dry air masses. The composition of "background" air and the relation between measurements made near the surface and at higher altitude were also discussed.

In this article we obtain information on chemical and physical processing by considering the photochemical age of an air

[1]Environmental Chemistry Division, Brookhaven National Laboratory, Upton, New York.
[2]Cloud Physics Research Division, Atmospheric Environment Service, Downsview, Ontario, Canada.
[3]Aeronomy Laboratory, National Oceanic and Atmospheric Administration, Boulder, Colorado.
[4]Centre for Atmospheric Chemistry, York University, North York, Ontario, Canada.
[5]Deceased April 1, 1995.

Copyright 1996 by the American Geophysical Union.

Paper number 95JD03787.
0148-0227/96/95JD-03787$09.00

mass and the effects of vertical motion upon composition. Age estimates are derived from the ratios of light hydrocarbons and are used to divide the Twin Otter data set into four age groups. Vertical profiles of O_3 and dew point and the relations between O_3 and other trace constituents are then examined as a function of photochemical age. Differences in the chemical composition of moist and dry air masses are discussed in terms of the selective removal of soluble constituents during vertical lifting. This discussion is based on the observed relation between aerosol particles and water vapor.

Effects of aging and vertical motions are illustrated using data from four case study periods in which elevated levels of O_3 occurred. The four cases span a wide range of conditions; photochemical ages vary from among the most recent to well aged; dew points vary from −20° to 17°C; and in one case the elevated O_3 appears to be associated with a biomass burning plume.

2. Experiment

Part 1 contains a list of flights and a description of the Twin Otter aircraft and its chemical instrumentation. We note here briefly that O_3 was determined by UV absorption, NO_y by chemiluminescence following reduction by a heated Mo converter, CO by gas filter correlation, and aerosol number concentration by a Particle Measurement Systems (PMS) PCASP probe (dry diameter 0.12–3 μm). All chemical data are expressed in mixing ratio units, either parts per billion by volume (ppbv) or parts per trillion by volume (pptv) for the gases or number per standard cubic centimeter for aerosol particles. Data have been averaged over 30-s time intervals and in some cases (as indicated) further averaged over 200 m altitude bins or over the several minutes it takes to collect a hydrocarbon sample.

Air samples for hydrocarbon analysis were collected into 6-L electropolished stainless steel canisters (Biospherics Research Corporation, Oregon), pressurized by means of a stainless steel bellows pump. Canisters were sent to the field evacuated. Sample collection entailed partially filling and then venting the canister to condition it before the final sample collection.

Canisters were returned to York University for analysis. C2–C6 hydrocarbons were measured using gas chromatography and flame ionization detection. Separation was performed on a 50-m × 0.32-mm Al_2O_3/KCl PLOT column. Sample sizes of 1.5 L were preconcentrated after passing sequentially through a trap filled with 5 g of K_2CO_3 held at 80°C to remove CO_2 and a 15-cm length of Teflon tubing cooled with dry ice to −50°C to further reduce the water content. Ambient samples and standards run through this system showed no losses for C2–C7 alkanes and alkenes, acetylene, benzene, and toluene. Blanks, consisting of ultrapure, hydrocarbon-free helium, were periodically run between sample analyses. These were always clean with respect to the lowest concentrations observed, indicating no carryover from the CO_2 and H_2O traps. Replicate analyses, whereby canisters were reanalyzed a week or two after the first analysis, were performed over the analysis period to validate system and operator performance. Replicate analyses were always within a few percent of each other. The preconcentration system is described elsewhere [*Jobson*, 1994].

Calibration of individual hydrocarbon responses was done from a ppbv range gravimetric mixture prepared by Conservation and Protection Services of Environment Canada. Quantification limits (1 sigma uncertainty is 10%) were operationally defined from the observed relation between analysis precision and peak areas of ambient samples and prepared mixtures. Quantification limits vary slightly with hydrocarbon species. For C5 alkanes the quantification limit for a 1.5-L sample was calculated to be 3 pptv. The lowest observed concentrations of C5 alkanes were 5 pptv, slightly above the quantitation limit. This 5-pptv peak yields a signal 10 times greater than the baseline noise width. The corresponding detection limit is 1 pptv. For concentrations well above the quantitation limit the analysis precision is 1%–2%, and the overall analysis uncertainty, including uncertainty in calibration and sample size determination, is 5%.

One hundred and five HC samples were taken between flights 6 and 48. Canisters were filled during level flight segments, typically taking 5 min. Trace gas instruments were usually zeroed before or after the HC samples. Approximately half of the HC samples were obtained at flight altitudes which were selected prior to the flight, thus guaranteeing that samples would be obtained under a broad range of conditions. The other half of the samples were used for flight segments that were judged to be of particular interest on the basis of in-flight measurements. As a consequence, layers with high pollutant concentrations have more than their statistical share of HC samples.

3. Results and Discussion

In this section we consider the composition of air masses from the standpoint of their photochemical age and the processing that occurs during vertical lifting. Four high-O_3 events have been selected for individual examination and are presented as case studies. These events, occurring on flights 6–9, 22, 29, and 35, were chosen because they span a broad range of conditions associated with high O_3 levels. High-O_3 layers in flights 6–9 and 22 occur in dry air masses, while flights 29 and 35 occur in moist air masses.

3.1. Photochemical Age

We have used the ratios of the concentrations of the light hydrocarbons, propane, *n*-butane, and *i*-butane, to obtain photochemical age estimates. In this technique it is assumed that the relative abundances of a set of hydrocarbons varies with time, as the more reactive species disappear at a faster rate than the less reactive ones. Initial implementations of this technique considered only reaction of hydrocarbons with OH or Cl. Recent work has indicated that hydrocarbon ratios depend also on dilution effects.

Following *McKeen and Liu* [1993] and *McKeen et al.* [1996], the change in concentration of a hydrocarbon X with mixing ratio [X] is approximated as

$$d[\mathrm{X}]/dt = -L(x)[\mathrm{X}] - K([\mathrm{X}] - [\mathrm{X}^b]) \qquad (1)$$

where $L(x)$ is the rate of disappearance due to reaction with OH (i.e., k_x [OH]), K is a mixing coefficient which expresses the overall rate for the dilution of hydrocarbon containing source air with background air, and $[\mathrm{X}^b]$ is the background concentration of X. The definition of background can be problematic, as in some cases it is appropriate to consider relatively clean upper altitude air as background, while in other cases, background may consist of aged boundary layer air. In order to simplify the analysis, we restrict our attention to hydrocarbons for which the term $[\mathrm{X}^b]$ in (1) can be approximated as zero. In an effort to meet the zero background criteria but still utilize

compounds with concentrations well above detection limits, we consider the time evolution of propane (C_3), n-butane (n-C_4) and i-butane (i-C_4).

Applying (1) to a pair of hydrocarbons (i.e., n-C_4 and C_3) yields

$$[n\text{-}C_4] = C\,[C_3]^{(K+L(n\text{-}C_4))/(K+L(C_3))} \qquad (2)$$

where C is a constant dependent on the initial concentrations of n-C_4 and C_3. A similar expression relates the concentrations of i-C_4 and C_3. The slope of a ln-ln plot of n-C_4 versus C_3 (or i-C_4 versus C_3) thereby gives a relative measure of the contributions of mixing and chemical reaction to the disappearance of a hydrocarbon.

Equation (2) has been applied to the NARE data set. A linear least squares fit yields an r^2 correlation coefficient of 0.89 and slope of 1.404 for ln [n-C_4] versus ln [C_3] and values of 0.87 and 1.418 for ln [i-C_4] versus ln [C_3]. Using rate constants for OH + C_3, n-C_4, and i-C_4 [*Atkinson*, 1994] evaluated at an average temperature of 287 K, we obtain two predictions for the rate of dilution relative to chemical reaction. $L(n\text{-}C_4)$ is arbitrarily selected as a yardstick for OH reactivity. From the n-C_4 versus C_3 regression, $K/L(n\text{-}C_4) = 0.95$; from i-C_4 versus C_3, $K/L(n\text{-}C_4) = 0.72$. Thus dilution is almost as important as reaction with OH in determining the concentration of a hydrocarbon that reacts as rapidly as n-C_4. A slightly more important role for dilution was determined by *McKeen et al.* [1996] in their analysis of hydrocarbon samples collected during PEM-West, over the Pacific Ocean, downwind of the Asian continent. They obtained values for $K/L(n\text{-}C_4)$ of 1.20 and 1.14 from regressions of n-C_4 versus C_3 and i-C_4 versus C_3, respectively. McKeen et al. found that these dilution estimates were fairly insensitive to the existence of nonzero background hydrocarbon concentrations.

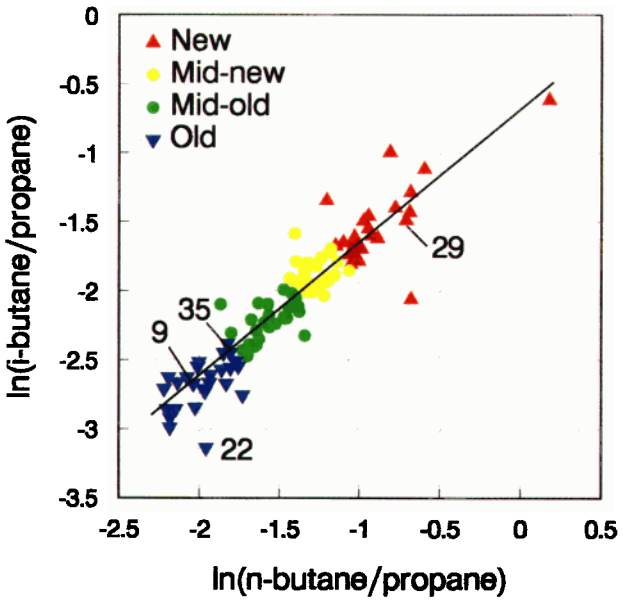

Plate 1. Photochemical age estimates based on the ratios ln (i-butane/propane) and ln (n-butane/propane). Data are split into quartiles of different photochemical age as discussed in text and specified in plate legend. Regression line ($r^2 = 0.87$) was calculated assuming equal errors in the ordinate and abscissa. Data points from four case study flights are indicated on the plate.

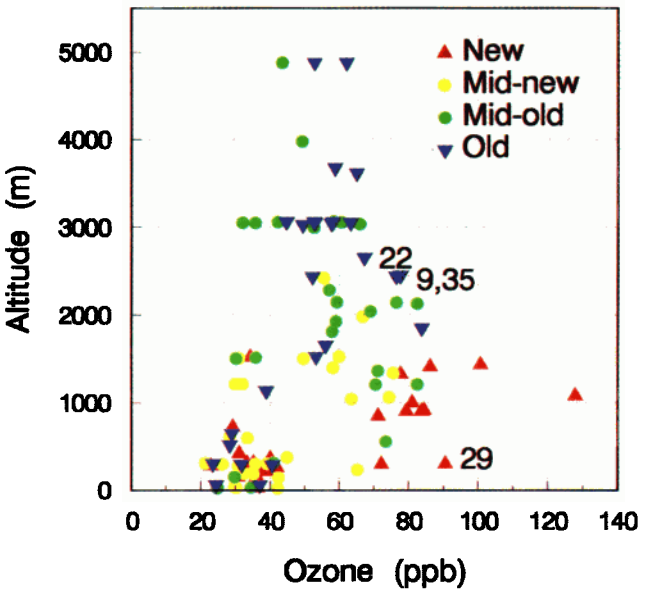

Plate 2. Ozone vertical profile. Measurements are coincident with hydrocarbon samples. Age estimates are derived from ratios of light hydrocarbons as shown in Plate 1 and specified in plate legend. Data points from four case study flights are indicated on the plate.

The change in ln [X] could be used as a marker for the degree of processing a plume has undergone. This quantity decreases monotonically with time, but the starting point for this "clock" depends on the emission strength of the source, i.e., the initial concentrations. A better index is the log of a hydrocarbon ratio, say, ln ([n-C_4]/[C_3]). This index also decreases monotonically with time but is less sensitive to initial concentrations. Some scatter in the ratio might be expected from differences in emission ratios arising from different sources.

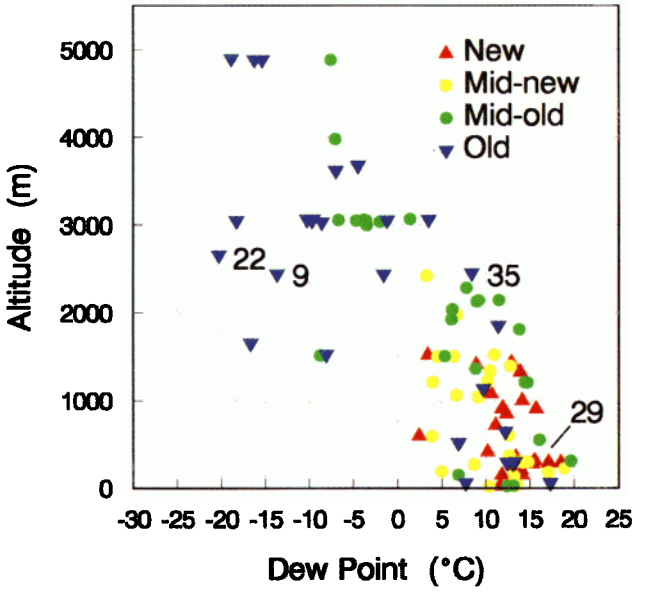

Plate 3. Dew point vertical profile. Format is the same as Plate 2.

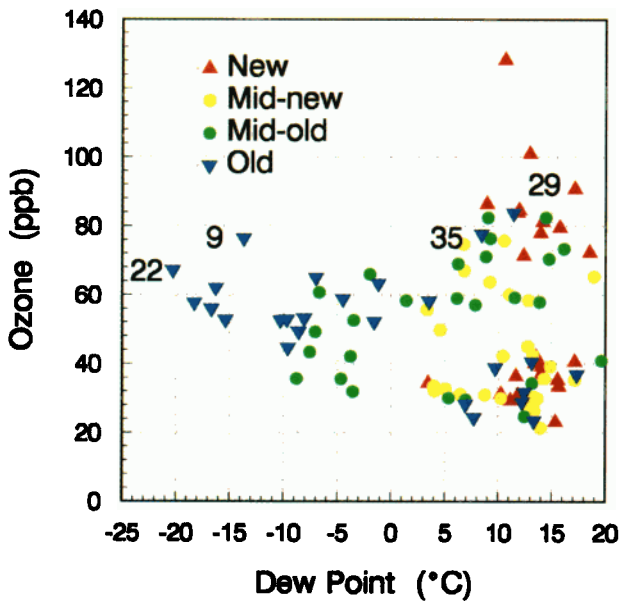

Plate 4. Relation between ozone and dew point. Format is the same as Plate 2.

In this paper the ratios ln ([n-C_4]/[C_3]) and ln ([i-C_4]/[C_3]) are used as indicators of "photochemical age," with the understanding that photochemical age reflects reaction and if "background" concentrations are significant, also dilution. This measure is somewhat imprecise, as samples can contain hydrocarbons from multiple source regions and the photochemical age is a convolution over the history of the air parcel. Because of this imprecision the hydrocarbon ratios will be used only in a qualitative way to provide an approximate ordering between new and old air masses. Toward this end we have divided the Twin Otter data set into quartiles of different photochemical age based on the rank order of ln ([i-C_4]/[C_3]) + ln ([n-C_4]/[C_3]). We will be referring to air masses by their age estimate as new, mid-new, mid-old, and old air. Back trajectories indicate that the old air masses with the lowest hydrocarbon ratios are approximately 3–5 days removed from their emission region.

Plate 1 shows the relation between ln ([i-C_4]/[C_3]) and ln ([n-C_4]/[C_3]), with data points color coded according to age estimate. There is a high correlation (r^2 = 0.87) between the two ratios, indicating that both ratios give similar age estimates. In addition, the slope of the least squares regression line conveys information on the relative rates of reaction of the three hydrocarbons [*McKeen et al.*, 1990, 1995; *Parrish et al.*, 1992, 1993; *McKeen and Liu*, 1993; *Jobson et al.*, 1994]. *McKeen and Liu* [1993] and *McKeen et al.* [1996] have shown that the slope m is independent of mixing and is given by

$$m = (L(i\text{-}C_4)\text{-}L(C_3))/(L(n\text{-}C_4)\text{-}L(C_3)), \qquad (3)$$

subject to the approximation that background levels of C_3, n-C_4, and i-C_4 can be ignored.

The least squares fit to the data in Plate 1, calculated assuming equal errors in the ordinate and abscissa, has a slope of 0.96, which is close to that predicted based on (3) using OH reaction kinetics (0.87 at 287 K) [*Atkinson*, 1994]. This agreement does not imply that the hydrocarbon concentrations are determined only by OH reactions. As previously demonstrated, dilution is of comparable importance as reaction. Furthermore, a slope near 1 could be produced by dilution if background levels of C_3 are significant. Cl atom reactions, however, yield a very different slope, and the agreement between theory and observations indicates that Cl reactions play at most a minor role in determining the time evolution of these hydrocarbons [*Parrish et al.*, 1993; *Jobson et al.*, 1994].

3.2. Relations Between Photochemical Age and Composition

Average values of chemical concentrations and meteorological parameters have been calculated over several-minute-long

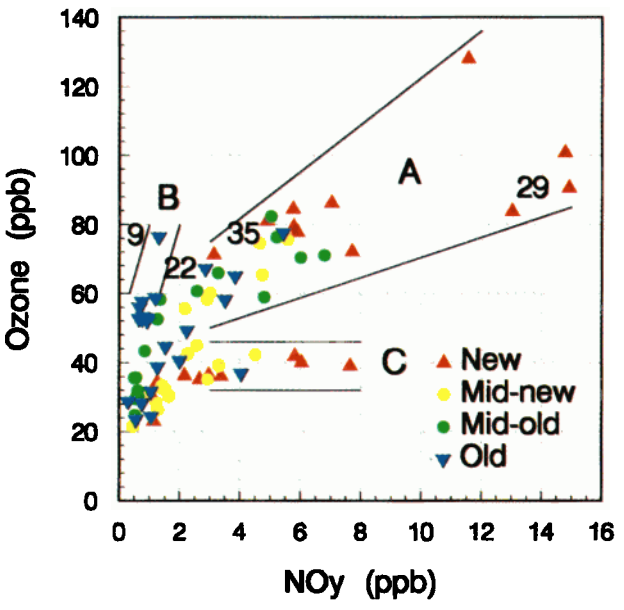

Plate 5. Relation between ozone and NO_y. Format is the same as Plate 2. Regions A, B, and C are defined by straight lines on graph. These regions correspond approximately to data points from moist plumes, dry plumes, and near-source region.

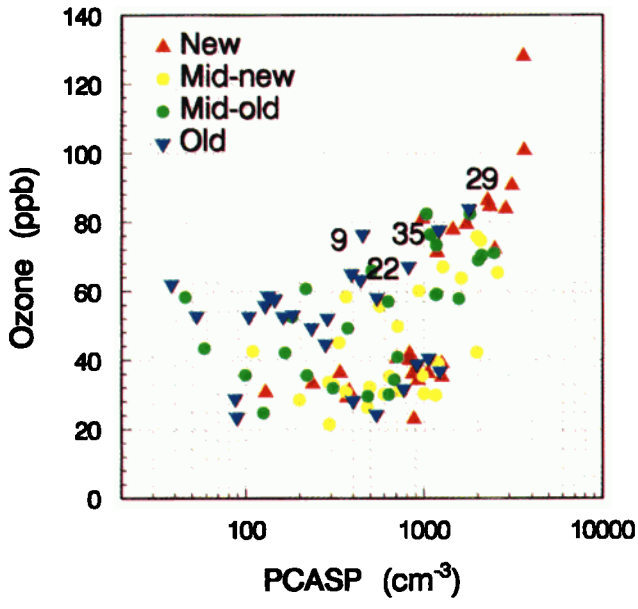

Plate 6. Relation between ozone and aerosol number concentration measured from PCASP. Format is the same as Plate 2.

time periods, coincident with the HC samples. These averaged values are shown in Plates 2–6, which display vertical profiles and relations between parameters with data symbols coded according to photochemical age. The range of chemical concentrations shown in these plates extends to higher values than presented in part 1, where averages were taken over 200 m altitude bins. Table 1 contains parameter values coincident with four HC samples taken in high-O_3 layers on the case study flights: 9, 22, 29, and 35. A comparison between flights 9 and 35 is of particular interest because both samples come from layers with similar O_3, altitude, and photochemical age, but have large differences in dew point and chemical composition.

Plates 2 and 3 show vertical profiles of O_3 and dew point, respectively. Both plates indicate vertical trends in age, with new air confined to the lowest 1.5 km and only old and mid-old air above 2.5 km. Old air also occurs at low altitude. A range of ages is expected at low altitude, reflecting variations in meteorological conditions which place our sampling location under the dominant influence of either nearby or distant emission sources. The absence of photochemically new air at high altitude might be due to the remoteness of emission sources. Plate 3 shows that dry air is photochemically old. All samples taken with dew points below 0°C were in the older two categories.

According to Plate 2, the highest O_3 levels (maximum value 128 ppb on flight 24) were observed in photochemically new air. At an O_3 concentration of 80 ppb, which is still characteristic of a polluted air mass, we have a combination of new and old ages. Near ground level, there is a group of samples with O_3 between 20 and 45 ppb, with no apparent relation between age and O_3 concentration. In this subset of the data the old points tend to have background concentrations of anthropogenic pollutants, while most of the new points were taken very close to local emission sources, which is reflected in elevated concentrations of SO_2, NO_y, and other primary pollutants.

The relation between O_3 and dew point, coded for photochemical age, is shown in Plate 4. This plate shows many of the same features seen in Figure 16 of part 1. In particular, in part 1 we identified a set of points with low NO_y in which O_3 concentration increased with decreasing dew point. A similar band is apparent in Plate 4 and is identified as being mostly photochemically old. A majority of the moist continental plume points discussed in part 1 (points with dew point >0°C and O_3 > 60 ppb) are in the two newer categories. However, there are nine points out of 25 that are in the older two categories, indicating that moist high-O_3 episodes are associated with a range of transport conditions. Plate 2 shows that there are two photochemically old samples from flights 9 and 35 with nearly identical O_3 concentration (~78 ppb) and altitude (~2450 m). Plate 4 and Table 1 show that these samples have dew points that differ by 22°C, placing one sample in the moist plume category and the other in the dry plume category.

Plates 5 and 6 illustrate relations between O_3 and NO_y and aerosol particles, trace substances which indicate the influence of anthropogenic emission sources. We first consider the O_3-NO_y relation, which has been shown for the whole data set in Figure 18 of part 1. We recall that this figure showed two branches. The branch containing dry plume points has a slope, $\Delta O_3/\Delta NO_y$, of ~30, as explicitly shown in a following section. The slope for the branch containing moist plume points varies with NO_y concentration from a value of ~10 at low NO_y to ~4 at high NO_y [*Daum et al.*, this issue]. Regions A and B in Plate 5 show schematically the combination of O_3 and NO_y concentrations corresponding to most of the moist and dry plume points, respectively, shown in Figure 18 of part 1. In addition, a third region labeled C is defined, in which O_3 is about 40 ppb and NO_y varies between 3 and 8 ppb.

Table 1. Parameter Values Coincident With Selected HC Samples

	Flight			
	9	22	29	35
Altitude, m	2442	2657	301	2452
O_3, ppb	76.4	67.2	90.6	77.6
Dew point, °C	−13.7	−20.3	17.1	8.4
NO_y, ppb	1.3	2.8	14.9	5.4
PCASP, cm^{-3}	450	817	3074	1211
CO, ppb	...[a]	207	390	153
C_2H_2, ppt	175	404	1073	211
ln (n-C_4/C_3)	−2.04	−1.96	−0.71	−1.81
ln (i-C_4/C_3)	−2.67	−3.14	−1.49	−2.45

[a]Missing data.

Plate 5 shows that the moist plume points in region A span a range of NO_y concentration from ~3 to 15 ppb. The four photochemically new samples with very high NO_y (greater than 11 ppb) also have high CO (280–390 ppb) and high C_2H_2 (710–1360 ppt), indicating a relatively near and polluted source region. One sample (flight 24, altitude of 1080 m) has an O_3 concentration significantly greater than the others, but the reason is not apparent. The HC sampling of dry plumes in location B is unfortunately restricted to a single sample from flight 9 at 1.3 ppb NO_y. We note that the large dew point difference between this sample and the moist sample from flight 35, previously discussed, is accompanied by a large difference in NO_y. Plate 5 contains an additional dry plume sample outside of region B at a somewhat higher NO_y (2.8 ppb) from flight 22. This latter sample is from a haze layer extending from 2400 to 2900 m and will be discussed as a case study.

Points in group C are mainly low-altitude samples taken near emission sources, including, but not limited to, Saint John. The near-source origin is reflected in the hydrocarbon ratios causing many of these points to be in the new category. It is somewhat surprising to see one older sample (NO_y ~ 4 ppb) in this grouping. It is from flight 29 at 60 m, which is discussed in a following section. The chemical composition of the air, other than the reactive hydrocarbons, suggests a local emission source, but the smoothness of the concentration fields and the meteorological conditions are more consistent with long-range transport.

Plate 6 shows the relation between O_3 and aerosol particle concentration in the same format as Figure 17 of part 1. Highest particle concentrations are seen to occur in photochemically new air. The dry and moist old points from flights 9 and 35 are again identified. Consistent with the results from part 1, the moist high-O_3 layer has higher particle concentrations than does the dry layer.

3.3. Water Vapor, Aerosol Particles, and the Origin of Dry O_3 Layers

Dry air masses, as encountered on flights 9 and 22, tend to have significantly lower concentrations of NO_y and aerosol particles as compared with moist air masses with a similar O_3

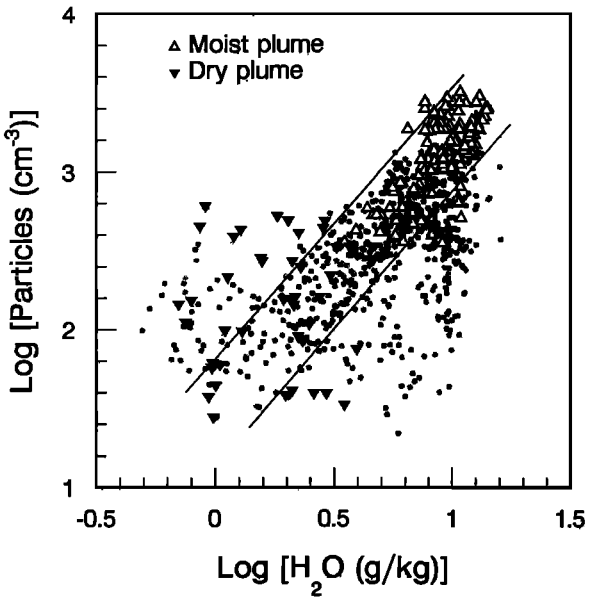

Figure 1. Correlation between the logarithm of aerosol number density measured via PCASP and the logarithm of water vapor mixing ratio. Data points are averaged over 200 m altitude bins in a single flight. Moist plume points have $O_3 > 60$ ppb and dew point >0°C. Dry plume points have $O_3 > 60$ ppb and dew point <−5°C. See part 1 for exceptions. Lines delineate a band containing most of the data.

concentration. The full data set presented in part 1 substantiates this observation. The relatively low NO_y and aerosol content of dry, high-O_3 layers introduces a potential ambiguity in determining the origin of these layers, as the possibility of an upper atmospheric source for O_3 must be considered. In this section we consider the physical factors which affect the concentrations of soluble substances such as water vapor, aerosol particles, and NO_y in order to gain insight into the origin of the dry, high-O_3 layers. NO_y is included among the soluble compounds since it is primarily HNO_3 according to the measurements of *Daum et al.* [this issue].

Vertical profiles of dew point and aerosol particle concentration, presented in part 1, indicate, on average, a steep and monotonic decrease with altitude. In previous work we have noted a mechanistic reason why aerosol particle and water vapor concentration decrease with altitude at about the same rate [*Kleinman and Daum*, 1991]. In brief, both substances have a surface or near-surface source, and both are removed from the atmosphere by precipitation scavenging. When air is lifted from the boundary layer, it cools, clouds form, and if the lifting is sustained and there is not significant dilution from upper altitude air, most of the water vapor will be removed as precipitation. Because soluble substances enter cloud water upon condensation, the lifting of boundary layer air to the middle or upper troposphere must be accompanied by a large decrease in the concentration of aerosol particles and soluble trace gases. If dilution occurs (as is usually the case to some degree and as is indicated by the hydrocarbon ratios previously discussed), then the mixing in of dryer upper altitude air will lessen or eliminate condensation. The occurrence of a variable amount of dilution does not change the conclusion that it is impossible to transport high concentrations of soluble substances from the boundary layer to the middle or upper troposphere. At the zero dilution extreme, low concentrations are caused by precipitation scavenging, whereas at the other extreme (i.e., no precipitation), dilution is directly responsible. An assessment of air mass origin based on aerosol particles as an anthropogenic tracer should therefore take into account the normal falloff with dew point. Low values of aerosol particles or soluble trace gases do not necessarily imply an upper atmospheric origin. In a similar spirit, *Fishman and Seiler* [1983] have analyzed the correlation of O_3 with other trace substances, taking into account the normal falloff with altitude.

Figure 1 shows water vapor and aerosol particle measurements averaged over 200 m altitude bins for flights 1–48. There is a large amount of scatter in the data, but a significant fraction of the measurements are confined to a band which has been drawn on the figure. Given that we expect a correlation between particles and water vapor, we propose a pragmatic definition whereby points in this band have an expected particle concentration, while points above and below have more or fewer particles, respectively, than expected. Lower than expected particle concentrations are in some cases due to particle removal mechanisms other than those associated with the concurrent removal of water vapor. For example, many of the data points below the band, at a water vapor concentration of about 10 g kg^{-1}, are in-cloud or close to the surface. Low particle concentrations could therefore be due to the transfer of particles to cloud droplets (which are not counted by the PCASP) or dry deposition. In other cases the low particle concentrations are measured in marine boundary layer air that has not been exposed to anthropogenic aerosol sources.

Data points corresponding to high O_3 concentrations are indicated on the figure. Following part 1, we separately consider dry high-O_3 layers (dew point is <−5°C) and moist high-O_3 layers (dew point is >0°C). We see that there is almost no overlap in particle concentration between the two types of high-O_3 events. On an absolute basis, particle concentrations are low in the dry subset, but relative to water vapor, most points are either in the expected concentration band or have more particles than expected. The one exception is flight 26 (altitude of 4–5 km), which contributes six points below the band.

Figure 1 does not identify the source of the O_3 in the dry high-O_3 layers because a particular combination of particle concentration and dew point can result from lifting boundary layer air to a higher altitude with or without mixing in high-O_3 upper altitude air. Nevertheless, we can obtain some insight into the origin of the O_3 in these layers based on the premise that all other things being equal, the sample with the higher particle concentration (at a given water vapor concentration) has the greater boundary layer influence. Points lying above the band in Figure 1, including samples from flights 6–9 and 22 discussed below, appear to have a boundary layer O_3 source based on C_2H_2 concentration and the correlations between O_3, NO_y, and aerosol particles. Points from flight 26 below the band and flight 28 at the lower left-hand corner of Figure 1 appear to have an upper altitude O_3 source based upon background-like hydrocarbon or CO concentration.

3.4. Case Studies

Dry, high-O_3 layer: Flights 6–9. A well-defined relatively dry layer at 2500 m with O_3 concentration reaching 80 ppb was observed on flights 6, 7, and 9 made on August 12 and 13. Conditions on flight 9, near the O_3 peak at 2500 m, are summarized in Table 1. The persistence of the layer at 2500 m, and

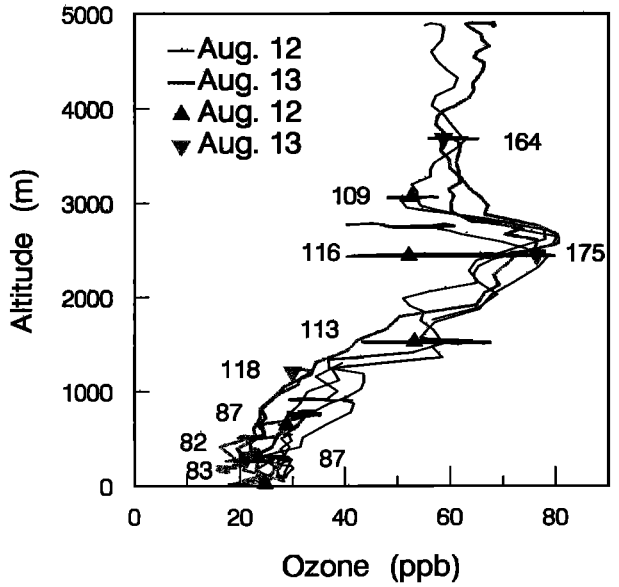

Figure 2. Ozone vertical profiles from flights 6–7 on August 12 and flights 8–9 on August 13, showing altitude and date of HC samples and C_2H_2 concentration.

that of the whole vertical column from the surface to 5 km, is shown in Figure 2. This figure also indicates the altitudes at which hydrocarbon samples were taken and the C_2H_2 that they contained. The high-O_3 layer at 2500 m is seen to have a C_2H_2 concentration that is significantly elevated with respect to "regional background" levels of 80–90 ppt [*Fan et al.*, 1994] which were observed below 1000 m.

The dew point within the high-O_3 layer was −15° to −20°C, approximately 20°C lower than occurred above or below this layer. Figure 3 shows that there is an overall anticorrelation between O_3 and dew point, with highest O_3 occurring in dry air.

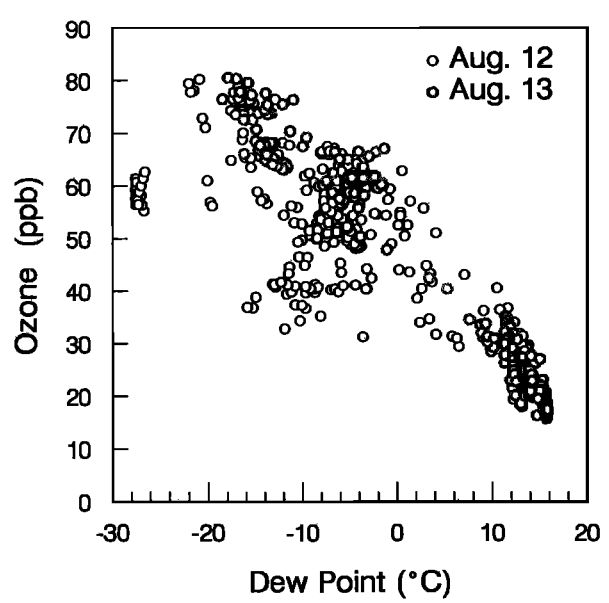

Figure 3. Scatter diagram showing an inverse relation between O_3 and dew point for measurements made on flights 6–9, August 12–13.

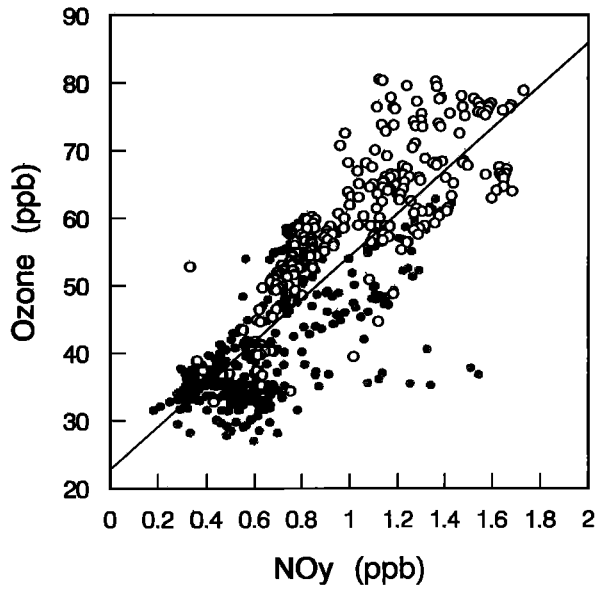

Figure 4. Scatter diagram showing a positive correlation between O_3 and NO_y in dry air with dew point <-5°C. Data are from flights 4–17, from the first flight with valid NO_y data to the end of the "clean period" described in part 1. Open circle data points are from flights 6–9; solid circles from flights 4–5 and 11–17. Data points with $O_3 > 60$ ppb come from air masses located at 2500 m on flights 6, 7, and 9, at 3–5 km on flights 6 and 9, and near 3 km on flights 5 and 11. Correlation for flights 4–17 is given in (4).

NO_y measurements, in contrast to dew point but in agreement with C_2H_2, indicate a boundary layer influence. Figure 4 indicates that the concentration of NO_y at peak O_3 is 1.8 ppb, which is relatively high for upper tropospheric air. This figure also shows that flights 6–9 are part of a larger data set in which the relation between NO_y and O_3 in dry air (dew point is <-5°C) can be expressed as

$$O_3\,(\text{ppb}) = 23 + 32\,NO_y\,(\text{ppb}), \qquad r^2 = 0.82. \qquad (4)$$

Ozone is correlated with NO_y with a slope that is less than found in upper tropospheric air [*Murphy et al.*, 1993], implying a source for NO_y in addition to that occurring in high-altitude air. Data in Figure 4 are restricted to measurements made in dry air, as moist air samples obey a different statistical relation (see Plate 5).

Differences between dry and moist layers can be seen in Table 1 where measurements from flight 9 are compared with data collected in a moist layer in flight 35 having similar O_3, altitude, and photochemical age. There is a 4.2- and 2.7-fold decrease in the concentration of NO_y and aerosol particles in dry air relative to moist air. According to Figure 1, the concentration of aerosol particles in the dry high-O_3 layer of flights 6–9 near 2500 m (N = 390–525 cm^{-3}), while low in absolute terms, is relatively high in comparison with water vapor (Q = 1.2–2.8 g kg^{-1}). The ratio of N to Q in this layer is almost an order of magnitude higher than found near the surface and severalfold higher than at the altitude where peak particle concentration occurs.

In contrast to the soluble constituents listed in Table 1, the C_2H_2 concentration at 2442 m (175 ppt) is comparable to that observed on flight 35 (211 ppt). CO is not available for flight 9,

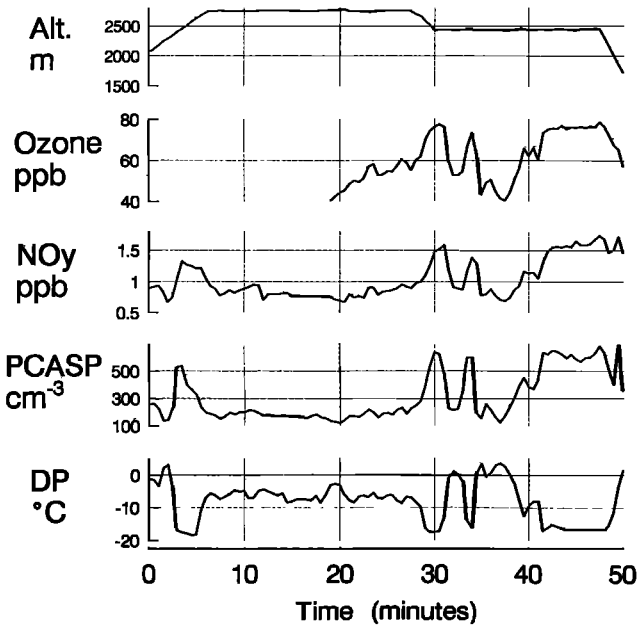

Figure 5. Fifty-minute time series from flight 7 for altitude, ozone, NO_y, aerosol number concentration (PCASP), and dew point. Twin Otter is circling over Chebogue Point at 2700 m and heading west over Gulf of Maine at 2500 m.

but the entire hydrocarbon data set indicates a correlation between CO and C_2H_2 given by

$$\mathrm{CO\ (ppb)} = 90.9 + 0.229\ C_2H_2\ \mathrm{(ppt)}, \quad r^2 = 0.67, \qquad (5)$$

which yields a CO estimate of 131 ppb for flight 9, which can be compared with 153 ppb measured on flight 35 (and 139 ppb deduced from C_2H_2). In comparing the high-O_3 layers in flights 9 and 35, we note that a similarity in the concentration of insoluble constituents and large differences in the concentrations of soluble substances is consistent with the selective removal of soluble substances during vertical transport. This does not imply that there is no dilution, only that dilution of boundary layer air on flight 9 is comparable to that occurring on flight 35.

The importance of dilution in determining the composition of older air masses is indicated, in general, by the quantities ln (n-C_4)/ln (C_3) and ln (i-C_4)/ln (C_3). We also note that air masses in the new and mid-new categories with a comparable O_3 concentration to that found in flight 9 have a C_2H_2 concentration centered at a value of ~400 ppt, about double that found on flight 9. Low concentrations of C_2H_2 in flights 9 and 35 are probably not due to chemical decay considering the lifetime of C_2H_2 but probably reflect mixing processes during transport.

While the anticorrelation between O_3 and dew point is suggestive of upper altitude air, the NO_y, C_2H_2, and particle data support a lower tropospheric origin for the elevated O_3. Back trajectories at 700 mbar are consistent with an aged anthropogenically influenced air mass (see Figure 15 in part 1). Possible emission regions are the Boston area, ~3 days upwind, and the Buffalo-Toronto region, ~5 days upwind.

Remnants of convection: Flight 7. There is a horizontal line at 2500 m in Figure 2 which corresponds to a constant altitude traverse in which O_3 concentration varied by tens of parts per billion over distances less than 5 km. Large variations in dew point at this altitude were also observed. These variations were observed on flight 7 and a day later on flight 9, but on the latter day, there is a smaller range in O_3 because the instrument was being zeroed during most of the traverse. We examine the nature of the small-scale variations in trace substance concentration in Figure 5, which is a time series for measurements made on flight 7 between 1800 and 2800 m altitude. This figure indicates that O_3 is positively correlated with NO_y and aerosol particles and anticorrelated with dew point. During the horizontal traverse at 2500 m, trace substance concentrations varied by a factor of 2 or more over distances of less than 5 km. The same sharply varying features were observed from the G-1 aircraft, which sampled along the same flight track as the Twin Otter as part of an intercomparison.

Large changes in dew point suggest that the variability shown in Figure 5 is due to convection which has displaced a portion of the dry high-O_3 air at 2500 m with moist low O_3 air from a lower altitude. Measurements of vertical wind velocity indicate that vertical exchange was not occurring to any appreciable extent during flight 7. The stability of the atmosphere at 2500 m would tend to inhibit the mixing of air parcels, and we propose that the structure at this altitude is a remnant of prior convective activity. Measurements with intermediate values of O_3 appear to be combinations of two air masses [*Paluch et al.*, 1992]: one that is dry with high pollutant concentration, the other moist with low pollutant concentration. Since mixing is a linear process, it contributes to the correlations between O_3, NO_y, particles, and dew point shown in Figures 3–5. The overall correlations expressed in Figures 3–5 and (4), however, are based on more than simple mixing, as multiple air masses were encountered on these flights.

Dry, haze layer: Flight 22. On August 23, flight 22, a visible haze layer was encountered in very dry air (dew point ~−20°C) at an altitude between 2600 and 2800 m. This layer, although having only a modest O_3 enrichment, had the highest concentrations of NO_y, CO, C_2H_2, and aerosol particles seen in dry air. Table 1 shows that concentrations of these substances are about a factor of 2 higher than observed in flight 9. Flight 22 contributes the NO_y data points previously noted in part 1 (see Figure 18) as being intermediate in concentration between that typically observed in low and high dew point air masses.

Particle mean volume diameter (D_v, measured by PCASP) for the accumulation mode aerosol in the haze layer was significantly greater than observed in either moist or dry air, except for instances where relative humidities approached 100%. Within the haze layer, D_v was 0.4 μm. Outside of the haze layer and on other flights, D_v was in the range 0.2–0.3 μm. The chemical composition of the aerosol on flight 22 was anomalous, containing an order of magnitude less SO_4^{2-} than expected, based on the correlation between SO_4^{2-} and particle number concentration in other samples [*Banic et al.*, this issue] and a relatively high concentration of black carbon [*Chylek et al.*, this issue]. Both the size and composition data are consistent with biomass burning. *Andreae et al.* [1994] report mean volume weighted particle size measurements in the range 0.2–0.4 μm (as determined by PMS ASASP) for aged biomass plumes; *Kaufman et al.* [1992] summarize composition data showing that S accounts for ~1% of PM 2.5 (particles smaller than 2.5 μm diameter), while graphitic and organic carbon accounts for ~10% and 50%, respectively. Trajectory information is also consistent with a biomass burning origin for the

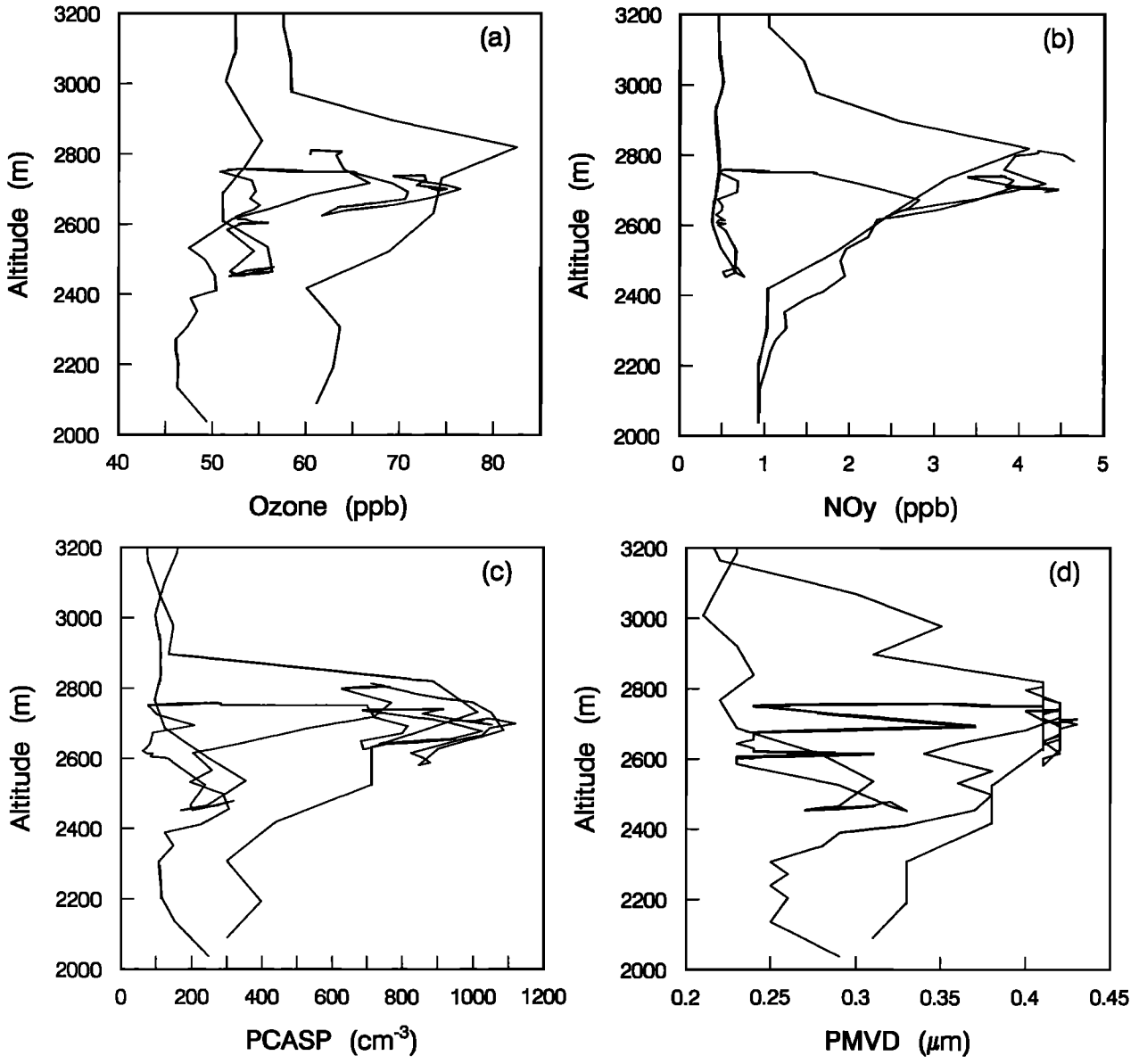

Figure 6. Vertical profiles through haze layer on flight 22 for (a) O_3, (b) NO_y, (c) particle number concentration from PCASP, and (d) volume weighted mean particle diameter from PCASP. Flight track is over the open ocean and Chebogue Point.

haze layer. Back trajectories at 850 and 700 mbar (see Figure 15 in part 1) traverse areas of Ontario that were responsible for forest fire plumes seen in ABLE 3B [*Shipman et al.*, 1994]. Climate Perspectives of Environment Canada indicate significant forest fires in Northwest Territories in early August 1993.

Figure 6 shows vertical profiles through the haze layer for O_3, NO_y, and aerosol particles. Air with "background" levels of these substances is seen to occur at the same altitude as the most polluted air. Sizable variations in pollutant concentration occur over distances as small as 5 km. In contrast to flight 7, variations in chemical concentration are not accompanied by significant changes in dew point, making it less likely that inhomogeneities are caused by convective activity. Horizontal gradients do not appear to be a result of recent emissions (i.e., aircraft exhaust), as the photochemical age estimate is in the old category and O_3 formation has occurred. Similar large horizontal gradients have been observed in aged biomass burning plumes by *Andreae et al.* [1994], lending weight to the possibility that the structure seen on flight 22 is a remnant of the initial emission pattern. There are small changes in temperature, dew point, and winds in the region where concentration is rapidly varying, and the possibility of a weak frontal surface should also be considered.

Continental plume: Flight 29. The moist continental plume that was intercepted by the Twin Otter on August 28, flight 29, was part of an extended pollutant layer that was observed by the KA and G-1 as far east as Sable Island [*Angevine et al.*, this issue; *Daum et al.*, this issue]. The surface site at Chebogue Point was also impacted. Within this episode, concentrations of O_3 and other trace substances were among the highest seen in the field campaign; O_3 concentrations close to 150 ppb were observed from the G-1. Parameter values near the point of maximum O_3 on flight 29 are summarized in Table 1.

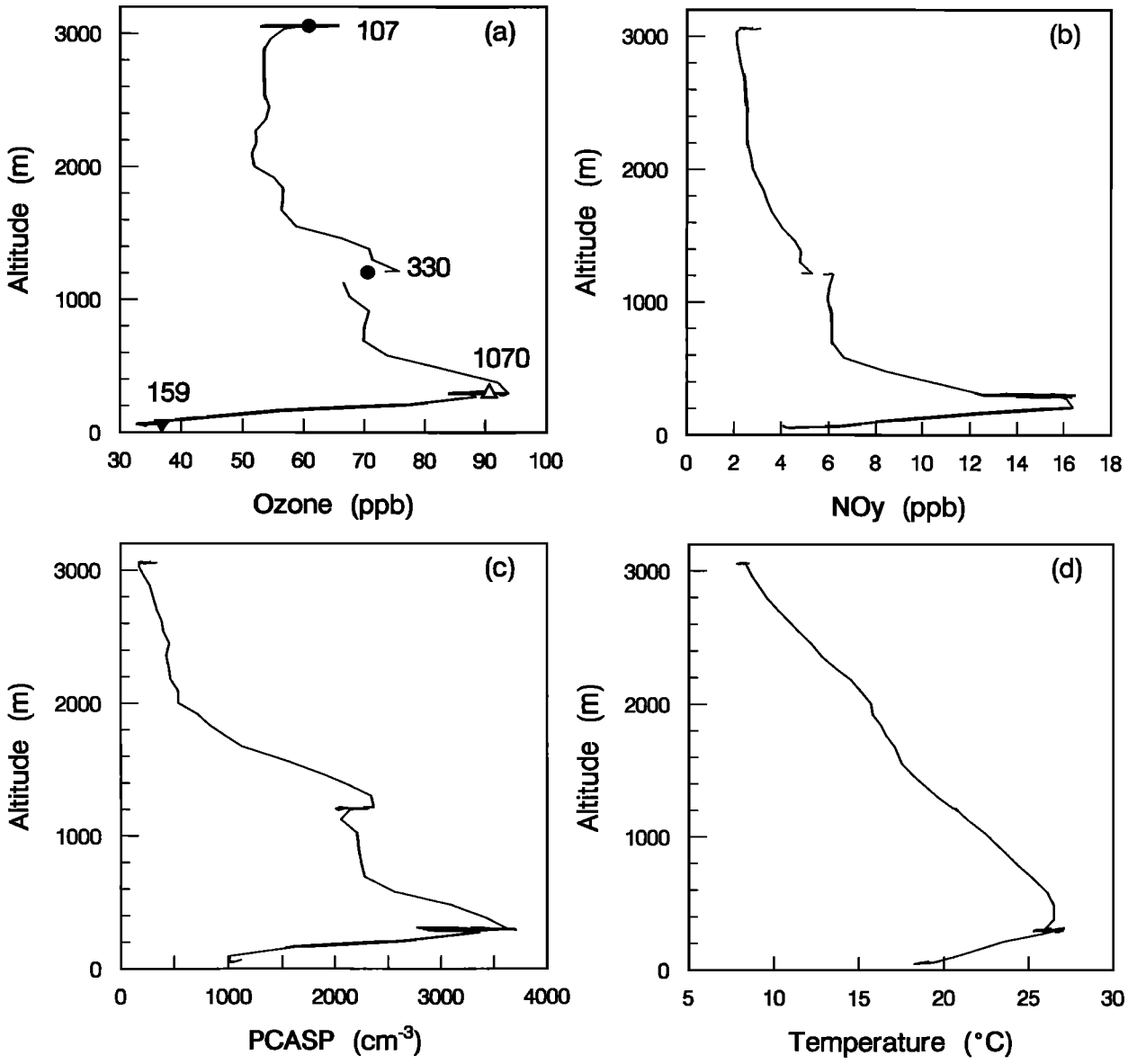

Figure 7. Vertical profiles from flight 29. (a) Ozone, showing age of HC samples and C_2H_2 concentration. HC ages are denoted by solid downward pointing triangle (old), solid circle (mid-old), and open upward pointing triangle (new). (b) NO_y. (c) Aerosol number density (PCASP). (d) Temperature. Flight track restricted to ocean locations 30–50 km south of Chebogue Point.

Vertical profiles of O_3, NO_y, and aerosol particles are shown in Figure 7. Locations of four hydrocarbon samples and values for C_2H_2 are also indicated. The spatial domain for this figure is restricted to an area more than 30 km south of Chebogue Point, as there were differences in composition between coastal and oceanic regions, particularly at low altitude. For example, near Chebogue Point, O_3 concentration at an altitude of 30 to 100 m was 50 ppb, whereas 40 km away at 60 m altitude the concentration was only 30 ppb.

According to Figure 7, the highest concentration part of the plume is at an altitude of 300 m and is only about 300 m deep. Above this thin layer is a region extending from 450 to 1200 m with somewhat lower O_3, NO_y, and particles, but still having a composition characteristic of moderately polluted continental boundary layer air. The temperature profile in Figure 7d indicates that maximum concentrations occur toward the top of a surface-based inversion layer. It was an unusual occurrence to find the continental plume within the surface inversion layer; plumes typically occurred above the inversion at somewhat higher altitude.

Within the inversion layer, there is a systematic shift in wind direction, changing from 265°–275° at 300 m to 230° at 60 m. Wind speed decreases from 15 m s^{-1} at 300 m to 9 m s^{-1} at 30 m. Wind shift will cause different emission regions to be upwind of our sampling location as a function of altitude and could account for the observed concentration gradients in the lowest 300 m. According to this scenario, surface air is cleaner than air at 300 m because it came from a region with lower emissions. Back trajectories provide support for this argument. The trajectory at 1000 mbar, shown in Figure 8, has a long fetch over water and just barely touches land at the tip of the Delmarva peninsula. The trajectory at 925 mbar runs just north

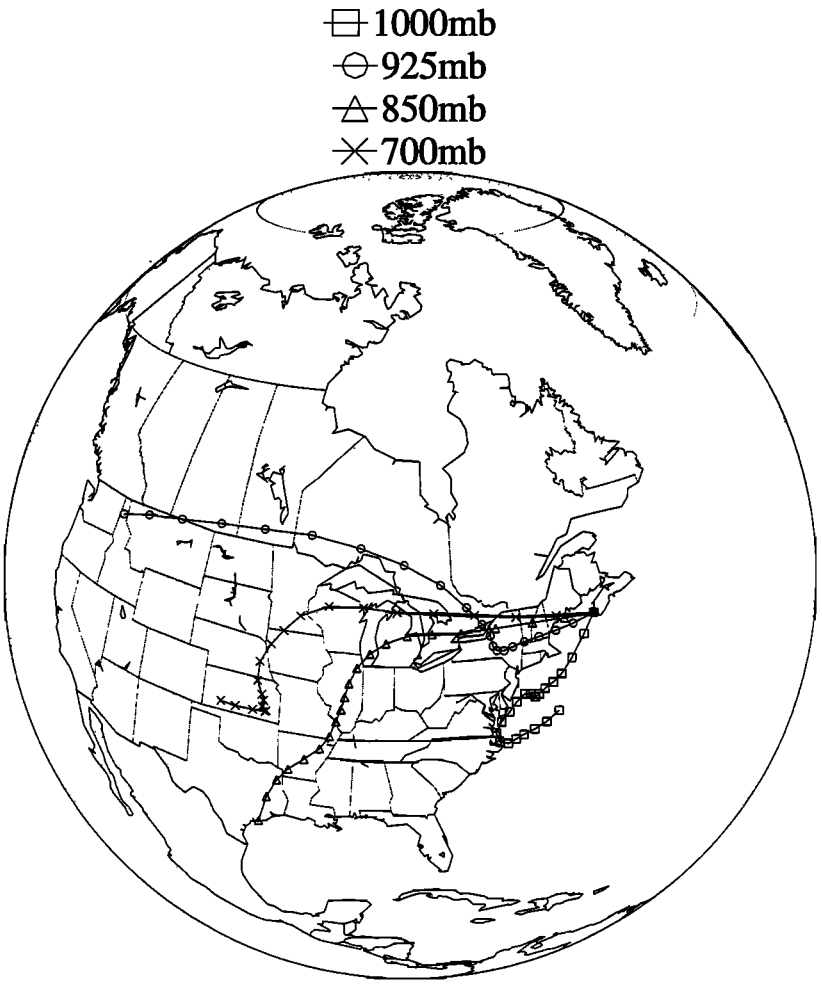

Figure 8. Five-day back trajectories at 1000, 925, 850, and 700 mbar terminating at Yarmouth Nova Scotia on August 28, 1200 UT. Segments are 6 hours apart. Trajectories have been calculated by the three-dimensional method of *Olsen et al.* [1978].

of Boston. By continuity and in accord with wind measurements from the Twin Otter, we expect that trajectories at intermediate altitudes fan out over the northeast corridor. Because of the stability of the atmosphere within the inversion layer, air parcels at different altitudes don't mix and thereby maintain a record of their independent origins. *Angevine et al.* [this issue] reach similar conclusions in interpreting vertical profiles observed from the KA.

The photochemical age estimate at 300 m is toward the young end of the new category. On the basis of this estimate and the travel speeds indicated by the Twin Otter wind measurements or by the trajectories in Figure 8, we believe that a source region at the northern end of the corridor accounts for the high pollutant concentrations at 300 m. From a preliminary analysis of NO measurements, we are able to determine that concentrations at 300 m were greater than 0.1 ppb. Coupled with high hydrocarbon concentrations as indicated by 1070 ppt C_2H_2 and 390 ppb CO, we expect that significant O_3 production is occurring at our measurement location.

Air at 60 m had a very different composition. An age estimate in the old category is consistent with a source region toward the south, several days travel time removed from Nova Scotia. Particle concentration (1230 cm^{-3}), NO_y (3.6 ppb), CO (167 ppb), and C_2H_2 (159 ppt) recorded during the HC sample at 60 m, while much lower than observed at 300 m, were higher than expected based on an O_3 concentration of 37 ppb. In other cases (see discussion of Plate 5) we have argued that this disparity is indicative of emissions from local sources that have not had a chance to form O_3. However, the sample from flight 29 is from a location 40 km south of Nova Scotia with the wind blowing from the southwest. The reason for low O_3 in this sample is not apparent.

The layer between 450 and 1200 m has a composition typical of moist air masses with O_3 levels of about 70 ppb. Above 1200 m the air is significantly dryer and contains lower levels of O_3, NO_y, and aerosol particles. At the point where the HC sample was obtained at 3000 m altitude, the composition of the air was typical of a dry (−6.7°C) high-O_3 (61 ppb) layer, being relatively depleted in NO_y (2.2 ppb) and aerosol particles (216 cm^{-3}). There is mixed evidence for selective removal of soluble constituents, as CO was high (201 ppb) but C_2H_2 was relatively low (107 ppt). Trajectories at 850 and 700 mbar indicate the possibility of impacts at these altitudes from sources near the Great Lakes region, Chicago, and the central United States. Age estimates are mid-old at 1200 and 3000 m.

Continental plume: Flight 35. Moist air with a continental boundary layer–like mixture of pollutants was observed on September 1, flight 35, over an altitude range extending from

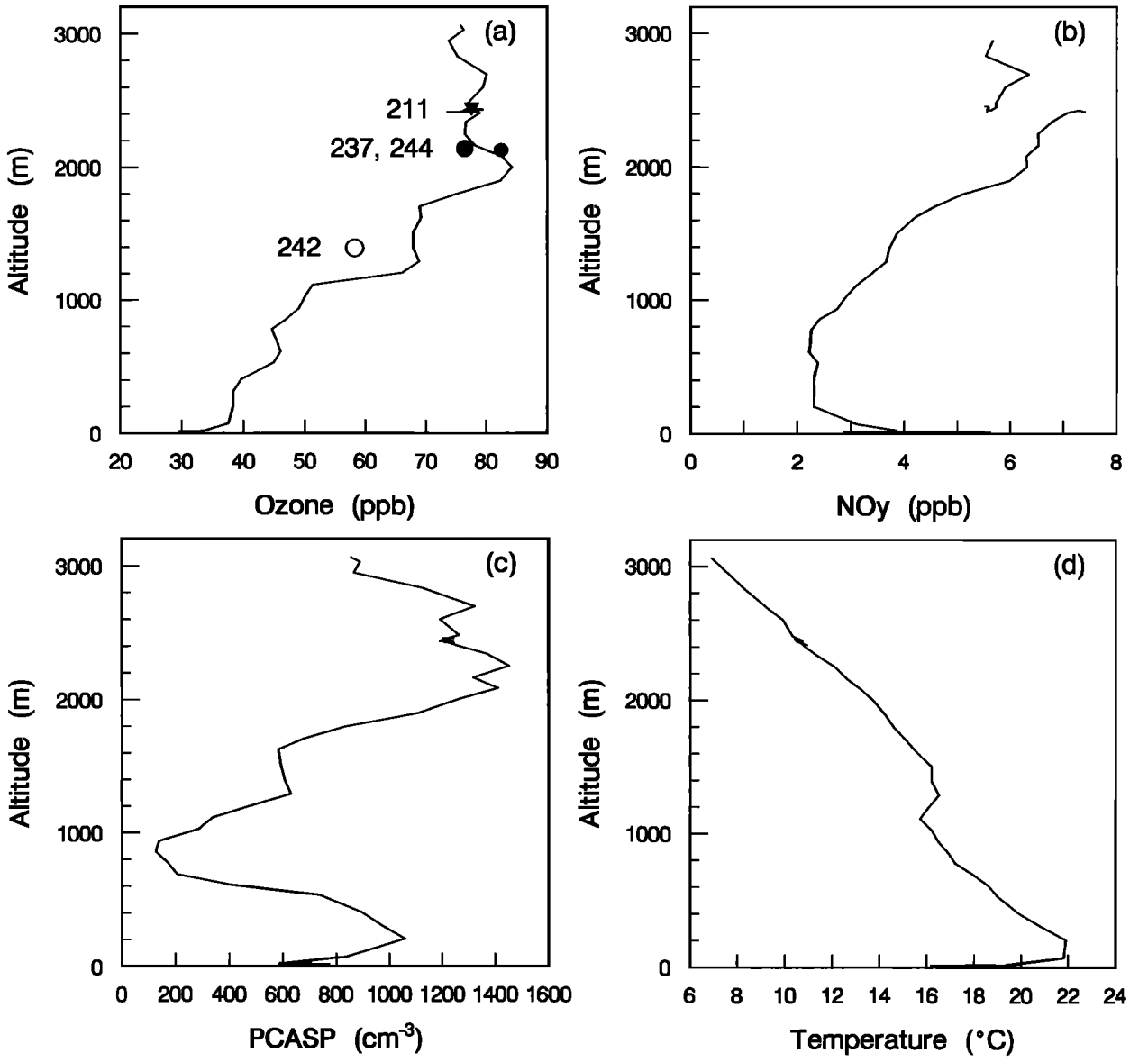

Figure 9. Vertical profiles from flight 35. (a) Ozone, showing age of HC samples and C_2H_2 concentration. HC ages are denoted by solid downward pointing triangle (old), solid circle (mid-old), and open circle (mid-new). (b) NO_y. (c) Aerosol number density (PCASP). (d) Temperature. Flight track is over Chebogue Point.

1300 m to the top of the sampling domain at 3000 m. The photochemical age observed in the continental layer at 2450 m was close to the oldest encountered in moist polluted air. In preceding sections we contrasted the composition observed on flight 35 with that observed on flight 9 in dry old air, finding that the concentration of insoluble material is similar on these two flights but that the concentration of soluble material is much lower on flight 9.

The chemical composition and temperature structure of the atmosphere above Chebogue Point is shown in Figure 9. As on several other flights the continental plume was defined from below by a temperature inversion which separated air masses having different source regions as judged by back trajectories or local wind measurements. Figure 7d indicates that there are two inversion layers: one at the surface and one at 1100–1300 m. There is an abrupt shift in wind direction at the same altitude as the second inversion. Below the inversion, winds are from the north-northeast (30°), whereas above, winds are from the west (270°). Differences in wind direction are reflected in the chemical composition, as shown in Figures 9a–9c. The air above the second inversion is seen to have significantly higher concentrations of O_3, NO_y, and particles as compared with the air below.

Locations of hydrocarbon samples and the corresponding C_2H_2 measurements are included in Figure 9a. Hydrocarbon-based ages range from mid-new at 1400 m to old at 2452 m. The hydrocarbon sample at 1400 m was collected 40 km inland from Chebogue Point, at which point the temperature inversion was shifted to higher altitude, placing this sample at the base of the inversion. The hydrocarbon measurements therefore identify the less polluted air below the inversion as being younger than the more polluted air above the inversion. Back

trajectories at 850 and 700 mbar indicate a possible upwind source region for the upper layer that includes most of the midwestern United States, with travel distances of order 3 days (see Figure 13 in part 1). We have ambiguous information on the origin of the air below the inversion. A back trajectory at 925 mbar indicates westerly flow with a possible source region in the midwest or southern United States. A trajectory several hours later indicates a possible influence from Yarmouth, consistent with wind measurements from the Twin Otter.

4. Summary and Conclusions

Using the trace gas and aerosol particle data set obtained from 48 flights of the NRC Twin Otter, we discuss the chemical content of the atmosphere over southern Nova Scotia, with particular reference to photochemical age estimates and physical changes that occur during transport. Four flights on which high O_3 concentrations were observed are presented as case studies.

Photochemical age estimates were determined based on the ratios *n*-butane/propane and *i*-butane/propane. Correlations between ln (butane) and ln (propane) indicated that dilution occurred almost as rapidly as the chemical removal of butane. A comparison between the two butane to propane ratios is consistent with OH being the primary oxidant.

Hydrocarbon ratios were used to divide the data set into quartiles of different photochemical age. Vertical profiles and relations between parameters were then examined as a function of age group. Hydrocarbon samples taken above 2.5 km were in the older half of the data set, as were all samples with dew points of <0°C. Air masses having the highest O_3 concentrations (i.e., greater than ~85 ppb) occurred in moist air and had high levels of other anthropogenic pollutants. Their photochemical age was in the "new" category, indicating transport of boundary layer air from nearby source regions in the coastal northeastern United States. Air masses with O_3 concentration between 60 and 85 ppb had a wide range of photochemical ages, consistent with transport times of order 1–5 days. Trajectory results indicate possible source regions in the coastal United States and relatively faraway areas in the interior of the United States and Canada.

Hydrocarbon sampling in dry high-O_3 air masses was sparse, but nevertheless offers some interesting comparisons with samples taken in moist high-O_3 air masses. Samples from flights 9 and 35 were compared, as they have similar photochemical age (old category), O_3 concentration (78 ppb), and altitude (2450 m), but differ in dew point by 22°C (−14° and +8°C, respectively). As found in part 1, the dry sample is relatively depleted in aerosol particles and NO_y. C_2H_2, in contrast, had about the same concentration in both samples. Differences in soluble constituents coupled with similarities in insoluble constituents was interpreted as evidence for the selective removal of soluble compounds by precipitation.

The low concentration of soluble substances, including aerosol particles and NO_y (which is largely HNO_3) found in dry high-O_3 air masses in general and flight 9 in particular, were interpreted in terms of the physical processing that is implied by the low concentration of water vapor. Movement of soluble substances from the moist boundary layer to the dryer free troposphere is strictly limited by a decrease in atmospheric temperature with altitude and the requirement that the moisture content of the lifted air eventually fall below saturation. This requirement can be met by diluting boundary layer air with dryer free tropospheric air or by the removal of water vapor in the form of precipitation. In either case, or in intermediate cases, soluble boundary layer substances share the same fate as boundary layer water vapor: either decreasing in concentration because of dilution or because of removal in precipitation. Low concentrations of NO_y and aerosol particles in dry high-O_3 layers are therefore a natural consequence of the vertical lifting of boundary layer air and do not necessarily imply an upper atmospheric origin for the O_3. A comparison of observed aerosol particle and water vapor concentrations shows that the concentration of aerosol particles in dry high-O_3 layers is relatively high in relation to water vapor, although low in absolute terms.

The four case studies illustrate the varying conditions under which high O_3 concentrations are observed. We discussed the following:

1. A persistent dry high-O_3 layer was observed on flights 6–9. Although O_3 was anticorrelated with dew point, an anthropogenic origin is indicated by the correlations between O_3, aerosol particles, and NO_y and by the relatively high concentration of (insoluble) C_2H_2. This sample was compared with a sample from flight 35, which had a clear boundary layer origin; differences were attributed to wet removal of aerosol particles and NO_y from the dry air mass.
2. A dry layer was observed on flight 22 that had an anomalous aerosol composition and particle size. A biomass burning origin is suspected, based on the low sulfur and high carbon content of the aerosol, as well as back trajectories.
3. A moist high-O_3 layer was observed at 300 m altitude on flight 29. This sample was located toward the top of a surface-based inversion. Its photochemical age was in the new category, and it had very high concentrations of all of the anthropogenic tracers that were measured. Air near the surface had a photochemical age in the old category and significantly lower pollutant concentrations. Back trajectories and wind measurements indicate a source region for the O_3 plume near Boston and a source region for surface air farther away, near the Delmarva peninsula. The stability of the atmosphere within the inversion layer prevented mixing.
4. A moist high-O_3 layer on flight 35 was observed between 1300 and 3000 m altitude. The photochemical age of this air mass was in the old category, similar to flight 9 and consistent with back trajectories passing over the midwestern United States. The chemical composition and dew point indicate that this was a lifted section of continental boundary layer air.

Acknowledgments. We dedicate this paper to the memory of our dear colleague, mentor, and friend, Hiromi Niki. The authors gratefully acknowledge a job well done by the ground and flight crews of the NRC Twin Otter. The many contributions of Steve Basic of AES and Paul Klotz, Jai Lee, Dan Leahy, Linda Nunnermacker, Judy Weinstein-Lloyd, and Xianliang Zhou of BNL to the measurement campaign are gratefully acknowledged. A special thanks to Mark Couture of AES for help in data processing. We would like to thank the personnel at Yarmouth Airport for their hospitality and expert assistance. We also appreciate the accurate weather forecasts provided by AES at Yarmouth. Stuart McKeen of NOAA contributed valuable comments on the interpretation of hydrocarbon ratios. This study was supported by funds from AES, NOAA, and the Atmospheric Chemistry Program of DOE. This paper has been authored under contract DE-AC02-76CH00016 with the U.S. Department of Energy under the Atmospheric Chemistry Program within the Office of Health and Environmental Research.

References

Andreae, M. O., B. E. Anderson, D. R. Blake, J. D. Bradshaw, J. E. Collins, G. L. Gregory, G. W. Sachse, and M. C. Shipman, Influence of plumes from biomass burning on atmospheric chemistry over the equatorial and tropical South Atlantic during CITE 3, *J. Geophys. Res.*, *99*, 12,793–12,808, 1994.

Angevine, W., M. Trainer, S. McKeen, and C. Berkowitz, Mesoscale meteorology of the New England coast, Gulf of Maine, and Nova Scotia: Overview, *J. Geophys. Res.*, this issue.

Atkinson, R., Gas-phase tropospheric chemistry of organic compounds, *J. Phys. Ref. Data, Monogr. 2*, 1994.

Banic, C. M., W. R. Leaitch, G. A. Isaac, M. D. Couture, L. I. Kleinman, S. R. Springston, and J. I. MacPherson, Transport of ozone and sulphur to the North Atlantic atmosphere during the North Atlantic Regional Experiment, *J. Geophys. Res.*, this issue.

Chylek, P., C. M. Banic, P. A. Damiano, G. A. Isaac, B. Johnson, W. R. Leaitch, P. S. K. Liu, D. Ngo, F. Said, S. R. Springston, and B. Winter, Black carbon: Atmospheric concentration and cloud water content measurements over southern Nova Scotia, *J. Geophys. Res.*, this issue.

Daum, P. H., L. I. Kleinman, L. Newman, W. Luke, J. Weinstein-Lloyd, C. M. Berkowitz, and K. Busness, Chemical and physical properties of plumes of anthropogenic pollutants transported over the North Atlantic during the North Atlantic Regional Experiment, *J. Geophys. Res.*, this issue.

Fan, S.-M., D. J. Jacob, D. L. Mauzerall, J. D. Bradshaw, S. T. Sandholm, D. R. Blake, H. B. Singh, R. W. Talbot, G. L. Gregory, and G. W. Sachse, Origin of tropospheric NO_x over subarctic eastern Canada in summer, *J. Geophys. Res.*, *99*, 16,867–16,877, 1994.

Fehsenfeld, F. C., A. Volz-Thomas, S. Penkett, M. Trainer, and D. D. Parrish, NARE 1993 summer intensive: Foreword, *J. Geophys. Res.*, this issue (a).

Fehsenfeld, F. C., P. Daum, W. R. Leaitch, M. Trainer, D. D. Parrish, and G. Hubler, Transport and processing of O_3 and O_3 precursors over the North Atlantic: An overview of the 1993 NARE summer intensive, *J. Geophys. Res.*, this issue (b).

Fishman, J., and W. Seiler, Correlative nature of ozone and carbon monoxide in the troposphere: Implications for the tropospheric ozone budget, *J. Geophys. Res.*, *88*, 3662–3670, 1983.

Jobson, B. T., Seasonal trends of nonmethane hydrocarbons at remote boreal and high arctic sites in Canada, Ph.D. thesis, York Univ., Toronto, Ont., Canada, 1994.

Jobson, B. T., Z. Wu, H. Niki, and L. A. Barrie, Seasonal trends of isoprene, C_2-C_5 alkanes, and acetylene at a remote boreal site in Canada, *J. Geophys. Res.*, *99*, 1589–1599, 1994.

Kaufman, Y. J., A. Setzer, D. Ward, D. Tanre, B. N. Holben, P. Menzel, M. C. Pereira, and R. Rasmussen, Biomass Burning Airborne and Spaceborne Experiment in the Amazonas (BASE-A), *J. Geophys. Res.*, *97*, 14,581–14,599, 1992.

Kleinman, L. I., and P. H. Daum, Vertical distribution of aerosol particles, water vapor, and insoluble trace gases in convectively mixed air, *J. Geophys. Res.*, *96*, 991–1005, 1991.

Kleinman, L. I., P. H. Daum, Y.-N. Lee, S. R. Springston, L. Newman, W. R. Leaitch, C. M. Banic, G. A. Isaac, and J. I. MacPherson, Measurement of O_3 and related compounds over southern Nova Scotia, 1, Vertical distributions, *J. Geophys. Res.*, this issue.

McKeen, S. A., and S. C. Liu, Hydrocarbon ratios and photochemical history of air masses, *Geophys. Res. Lett.*, *20*, 2363–2366, 1993.

McKeen, S. A., M. Trainer, E.-Y. Hsie, R. K. Tallamraju, and S. C. Lin, On the indirect determination of atmospheric OH radical concentrations from reactive hydrocarbon measurements, *J. Geophys. Res.*, *95*, 7493–7500, 1990.

McKeen, S. A., S. C. Liu, E.-Y. Hsie, X. Lin, J. D. Bradshaw, S. Smyth, G. L. Gregory, and D. R. Blake, Hydrocarbon ratios during PEM-West A: A model perspective, *J. Geophys. Res.*, *101*, 2087–2109, 1996.

Murphy, D. M., D. W. Fahey, M. H. Proffitt, S. C. Liu, K. R. Chan, C. S. Eubank, S. R. Kawa, and K. K. Kelly, Reactive nitrogen and its correlation with ozone in the lower stratosphere and upper troposphere, *J. Geophys. Res.*, *98*, 8751–8773, 1993.

Olsen, M. P., K. K. Oikawa, and A. W. MacAfee, A trajectory model applied to the long-range transport of air pollutants, *Rep. LRTAP 78-4*, Atmos. Environ. Serv., Air Qual. Res. Branch, Downsview, Ont., Can., 1978.

Paluch, I. R., D. H. Lenschow, J. G. Hudson, and R. Pearson, Jr., Transport and mixing processes in the lower troposphere over the ocean, *J. Geophys. Res.*, *97*, 7527–7541, 1992.

Parrish, D. D., C. J. Hahn, E. J. Williams, R. B. Norton, F. C. Fehsenfeld, H. B. Singh, J. D. Shetter, B. W. Gandrud, and B. A. Ridley, Indications of the photochemical histories of Pacific air masses from measurements of atmospheric trace species at Point Arena, California, *J. Geophys. Res.*, *97*, 15,883–15,901, 1992.

Parrish, D. D., C. J. Hahn, E. J. Williams, R. B. Norton, F. C. Fehsenfeld, H. B. Singh, J. D. Shetter, B. W. Gandrud, and B. A. Ridley, Reply, *J. Geophys. Res.*, *98*, 14,995–14,997, 1993.

Shipman, M. C., A. S. Bachmeir, D. R. Cahoon, Jr., G. L. Gregory, B. E. Anderson, and E. V. Browell, Meteorological interpretation of the Arctic Boundary Layer Expedition (ABLE) 3B flight series, *J. Geophys. Res.*, *99*, 1645–1657, 1994.

C. M. Banic, G. I. Isaac, and W. Richard Leaitch, Cloud Physics Research Division, Atmospheric Environment Service, Downsview, Ontario, Canada M3H 5T4.

P. H. Daum, L. I. Kleinman, and S. R. Springston, Environmental Chemistry Division, Brookhaven National Laboratory, P.O. Box 5000, Upton, NY 11973.

B. T. Jobson, Aeronomy Laboratory, National Oceanic and Atmospheric Administration, Boulder, CO 80303.

(Received May 5, 1995; revised December 8, 1995; accepted December 8, 1995.)